Lab 3 : Vehicle vibration control by using PD, PID, Skyhook and H^{∞} controllers

SD2231– Applied vehicle dynamics control

June 10, 2025

Group 4
Simon Loriot
Carlo Vittorio

Postal address
Royal Institute of Technology
KTH Vehicle Dynamics
SE-100 44 Stockholm
Sweden

Visiting address
Teknikringen 8
Stockholm

Telephone
+46 8 790 6000
Telefax
+46 8 790 9304

Internet
www.ave.kth.se

Contents

1 Testing scenarios

For every considered system, the response to three different scenarios have been tested:

- a sinusoidal excitation (amplitude 0.1, frequency 6.2rad/s)
- an impulse excitation (amplitude 0.05, duration 0.1s)
- a measured road excitation of power spectral density of $S_w(\omega) = \dfrac{4.028 \cdot 10^{-7}}{\omega^4 + 0.68\omega^2 + 2.88 \cdot 10^{-4}}$. The road power spectral density is represented figure 1. For this scenario, only the power spectral density of the response will be studied.

Figure 1: Power spectral density of the measured road excitation

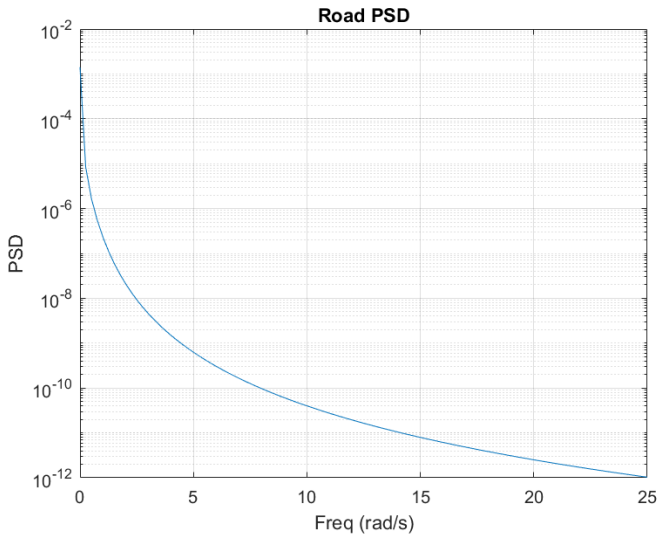

2 Control of a single DOF system using PD,PID and Skyhook

2.1 Uncontrolled system

In this part, vibration of a single degree of freedom system will be studied. This system is a simple mass with a spring and a damper, represented figure 2.

Figure 2: One degree of freedom system

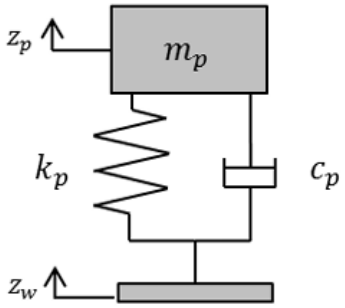

If we define the natural frequency $\omega_n = \sqrt{\frac{k_p}{c_p}} \approx 6.28 rad/s$ and damping ratio $\zeta = \frac{c_p}{2\sqrt{k_p m_p}} \approx 0.19$. We obtain equation (1), which represents the dynamic.

$$\ddot{z_p} = -\omega_n^2(z_p - z_w) - 2\zeta\omega_n(\dot{z_p} - \dot{z_w}) \tag{1}$$

A transfer function H_1 (can also be computed (2).

$$H(s) = \frac{Z_p}{Z_w} = \frac{2\zeta\omega_n s + w_n^2}{s^2 + 2\zeta\omega_n s + w_n^2} \tag{2}$$

The bode diagram of this system is represented figure 3.

Figure 3: Bode diagram of the uncontrolled one degree of freedom system

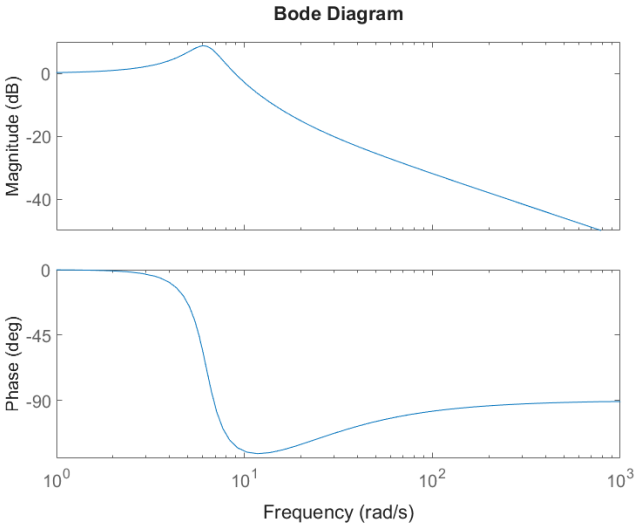

The bode diagram clearly shows a maximum in amplitude at $\omega = \omega_n\sqrt{1-\zeta^2}$. The frequency of maximum amplification if the system was not damped is the natural frequency of the system. To understand the meaning of the damping ratio, the response to a step was studied for three values of damping ratio : $\zeta \in \{0.5, 1, 2\}$. The system response is represented figure 4. For an underdamped system ($\zeta < 1$), the response will oscillates with a frequency of $w_d = w_n\sqrt{1-\zeta^2}$. For a critically damped system, the signal will reach the step as fast as possible without oscillations. For an overdamped system ($\zeta > 1$), the system will slowly reach the step without oscillations.

The response of scenarios 1 and 2 are represented figure 5; and the power spectral density of the response of scenario 3 is represented figure 6.

Figure 4: Response to a step excitation for different damping ratio

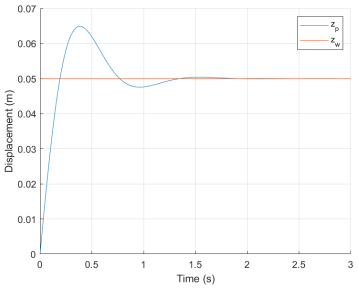

(a) $\zeta = 0.5$ under damped system

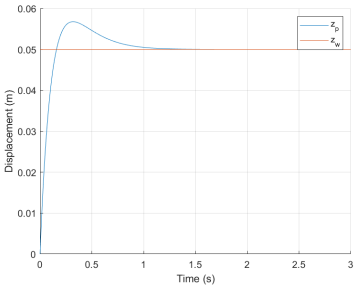

(b) $\zeta = 1$ critically damped system

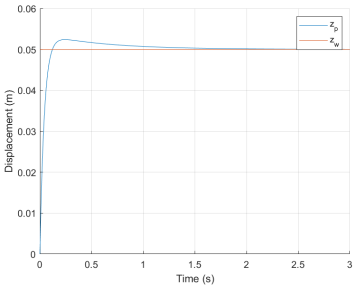

(c) $\zeta = 2$ over damped system

Figure 6: Power spectral density of the system responding to scenario 3

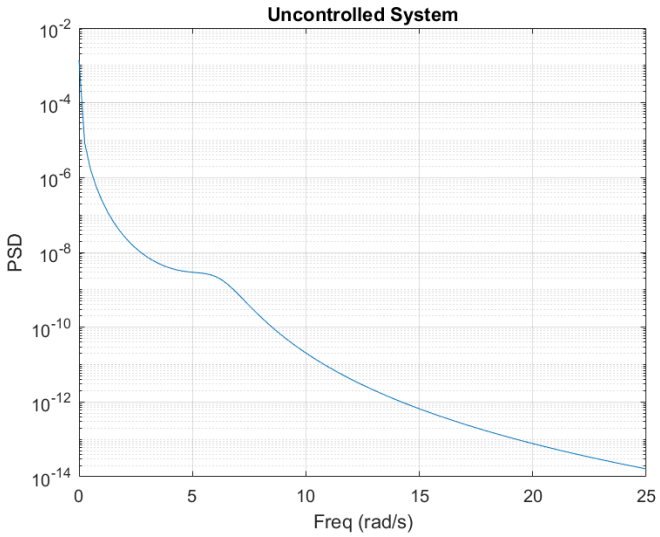

2.2 PD controller

The system can now be controlled by actively changed the value of c_p. The new system is represented figure 7.

Figure 5: Response to different inputs signals

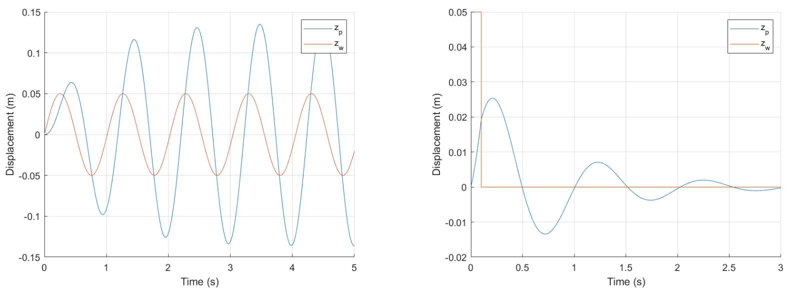

(a) Response to a sinusoidal signal (b) Response to an impulse

Figure 7: Controlled one degree of freedom system

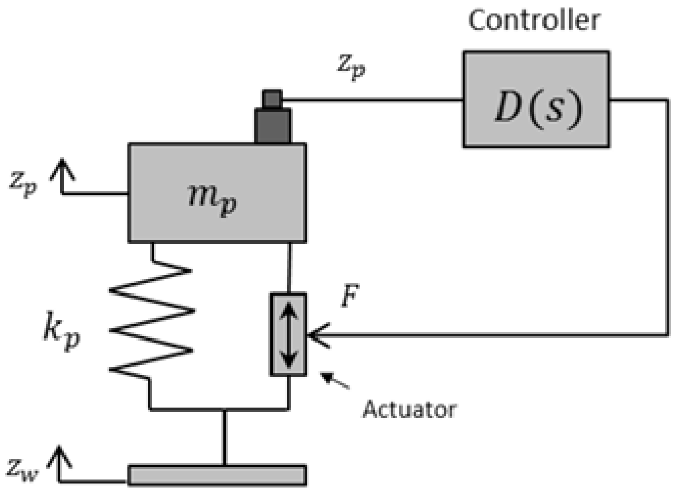

The first controller studied is a PD controller. The controller transfer function would be $D(s) = -(d_p + d_d s)$. We can derive the equation of motion (3) and the associated transfer function (4).

$$\ddot{z_p} = -\omega_n^2(z_p - z_w) - \frac{d_p}{m}z_p - \frac{d_d}{m}\dot{z_p} \tag{3}$$

$$H(s) = \frac{Z_p}{Z_w} = \frac{w_n^2}{s^2 + \frac{d_d}{m}s + \frac{k_p + d_p}{m}} \tag{4}$$

This transfer function is very similar to 2. For the parameters values $d_p = 0$ and $\frac{d_d}{m} = 2\zeta\omega_n$, the denominator are the same. Further tuning was made under the constraint that the system should stay underdamped and that the natural frequency of the system stay unchanged. The value $d_p = 0$ and $d_d = 1.3$ are found to be optimal for the different scenarios. The condition that the natural frequency of the system shouldn't change fixed the value of d_p. d_d was tuned to minimize the system amplitude in the sinusoidal signal, while keeping an underdamped system with the inpulse. The response to both excitation are represented figure 8.

Figure 8: Response to different inputs signals for the PD control

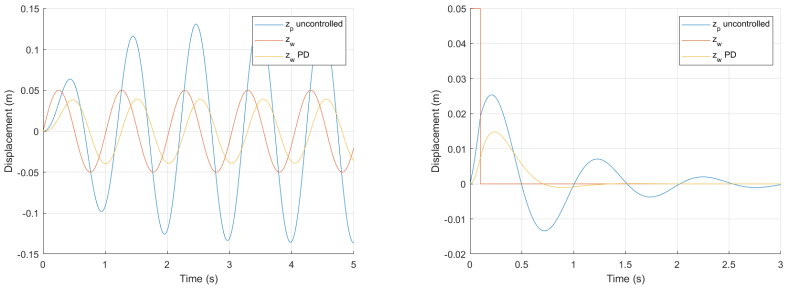

(a) Response to a sinusoidal signal

(b) Response to an impulse

The PD controller sucessfully reduces the maximum amplitude for both the impulse and the sinusoidal signal, while keeping the system underdamped and with the same natural frequency.

The power spectral density of the response to scenario 3 is represented figure 9. The controlled system reduces significantly the amplitude around the resonance frequency.

Figure 9: Power spectral density of the PD system responding to scenario 3

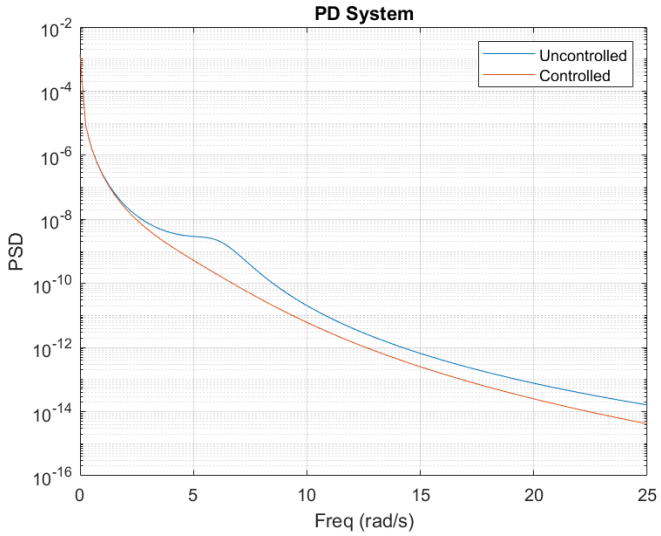

The value of critical damping is around $d_d \approx 1.5$. However, these value will make the vehicle very uncomfortable and sensitive to bumps.

2.3 PID

We now have a controlled signal $D(s) = -(h_p + h_d s + \frac{h_i}{s})$. The motion in time domain is the equation 5 and the transfer function is equation **??**.

$$\ddot{z_p} = -\omega_n^2(z_p - z_w) - \frac{h_p}{m}z_p - \frac{h_d}{m}\dot{z_p} - \frac{h_i}{m}\int_0^t z_p dt \tag{5}$$

$$H(s) = \frac{Z_p}{Z_w} = \frac{w_n^2 s}{s^3 + \frac{d_d}{m}s^2 + \frac{k_p + h_p}{m}s + h_i} \tag{6}$$

We can keep $h_p = 0$ to not change the natural frequency. After some tuning, the parameters $h_i = 14$ and $h_d = 3.5$ are optimal for the considered scenarios. The response for scenario 1 and 2 are represented figure 10.

Figure 10: Response to different inputs signals for the PID control

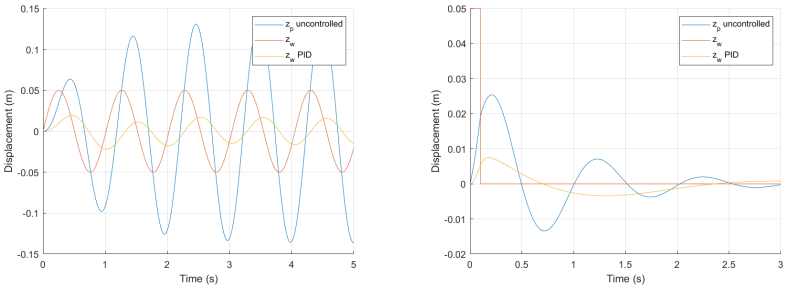

(a) Response to a sinusoidal signal

(b) Response to an impulse

The PID controller achieves better results than the PD controller. It reduces the amplitude of the excitation considerably, while keeping the natural frequency unchanged and the system is still underdamped. However, introducing a high h_i creates a steady state error. If our system encounter a step, the suspension system still returns to $z_s = 0$. It physically means that the equilibrium ride heigth is dynamic. To avoid this problem, a real life system must have an integral reset to avoid ride height change. The response to a step is represented figure 11.

Figure 11: Response of the PID system to a step

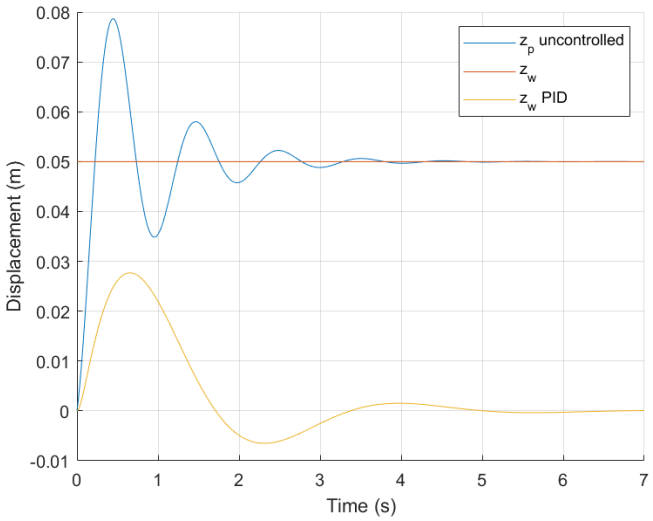

The power spectral density of the response to scenario 3 is represented figure 12. The controlled system reduces significantly the amplitude of very high and very low frequency compared to the PD system. However, just before the resonance around $\omega = 2rad/s$, the PD system performs better.

Figure 12: Power spectral density of the PID system responding to scenario 3

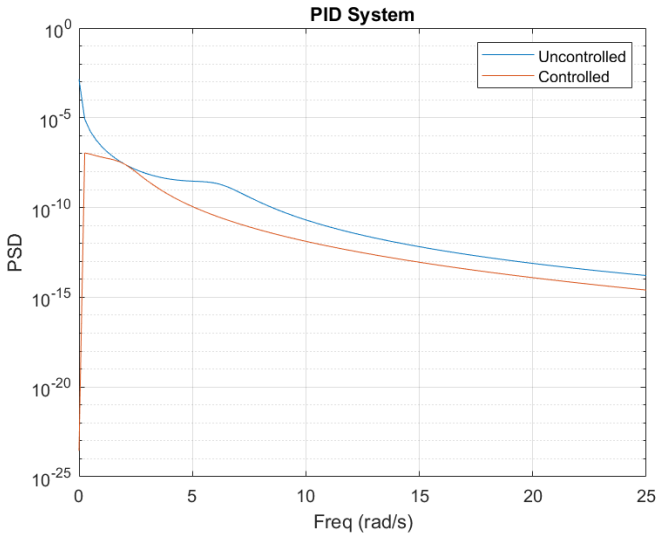

We can also consider F as an input signal. Therefore, we have

$$Z_p = Z_w \cdot \frac{w_n^2}{s^2 + w_n^2} + F \cdot \frac{\frac{1}{m}}{s^2 + w^2} \tag{7}$$

$$F(s) = D(s)Z_p \tag{8}$$

We can model the problem this way in Simulink, the plant would be :

$$A(s) = [\frac{w_n^2}{s^2 + w_n^2}, \frac{\frac{1}{m}}{s^2 + w^2}] \tag{9}$$

And we would have the plant equation :

$$Z_p(s) = A(s) \begin{bmatrix} Z_w \\ F \end{bmatrix} \tag{10}$$

We can model this system in simulink, represented figure 13. We have $u_1 = z_w$ and $u_2 = F$.

Figure 13: Simulink representation of the PID system

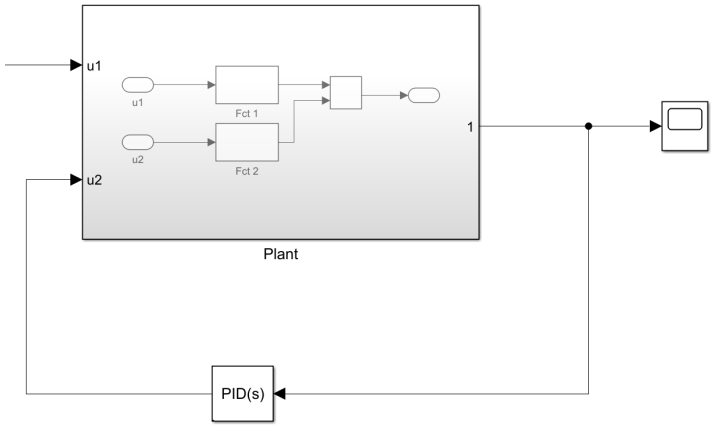

2.4 Skyhook controller

We now study the skyhook controller $D(s) = -Ts$. However, this controller is the same as the PD controller with $d_p = 0$. And as the tuned value of the PD controller is $d_p = 0$ (to not modify the natural frequency). The Skyhook controller is the exact same as the PD controller.

3 Control of a 2 DOF system using Skyhook

3.1 Damped passive system

In this section, a two degree of freedom model will be considered. The model is represented figure 14.

Figure 14: Two degree of freedom system

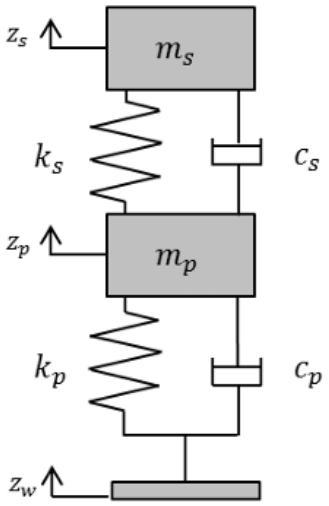

The equations of motion for this system are equations 11.

$$\begin{cases} m_s\ddot{z_s} = k_s(z_p - z_s) + c_s(\dot{z_p} - \dot{z_s}) \\ m_p\ddot{z_p} = k_p(z_w - z_p) + c_p(\dot{z_w} - \dot{z_p}) + k_s(z_s - z_p) + c_s(\dot{z_s} - \dot{z_p}) \end{cases} \tag{11}$$

From this equation, we can compute the transfer function of the system 12.

$$H(s) = \frac{Z_s}{Z_w} = \frac{\frac{c_s c_p}{m_s m_p}s^2 + \frac{k_s c_p + c_s k_p}{m_s m_p}s + \frac{k_p k_s}{m_s m_p}}{s^4 + (\frac{c_s + c_p}{m_p} + \frac{c_s}{m_s})s^3 + (\frac{k_s + k_p}{m_p} + \frac{k_s}{m_s} + \frac{c_s c_p}{m_s m_p})s^2 + \frac{s_p k_s + c_s k_p}{m_s m_p}s + \frac{k_p k_s}{m_s m_p}} \tag{12}$$

The bode diagram of this system is represented figure 15.

Figure 15: Bode diagram of the uncontrolled two degree of freedom system

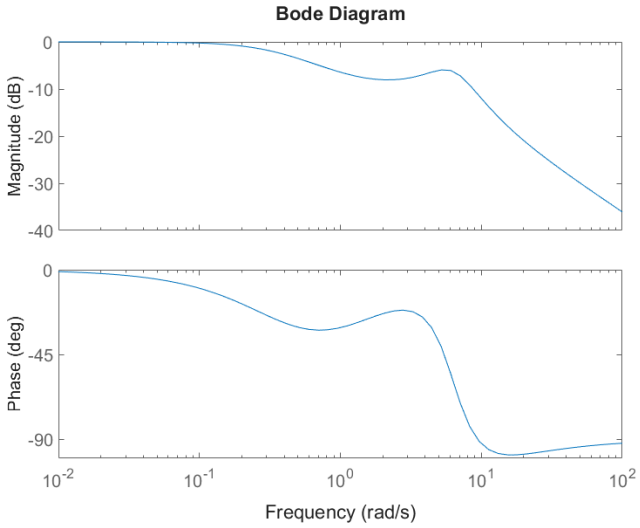

This bode diagram is very different from 3. First, the maximum amplitude is below 0db, therefore no frequency will be amplificated. Then, the two different natural frequencies can target a larger band of frequencies to be damped. The response to scenario 1 and 2 are represented figure 16. This system is already efficient to limit the amplitude of the response.

Figure 16: Response to different inputs signals for the uncontrolled 2DOF system

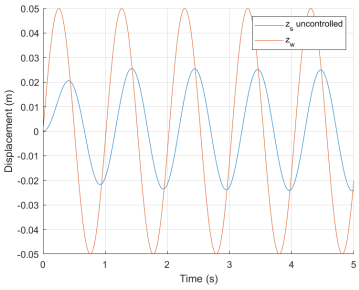

(a) Response to a sinusoidal signal

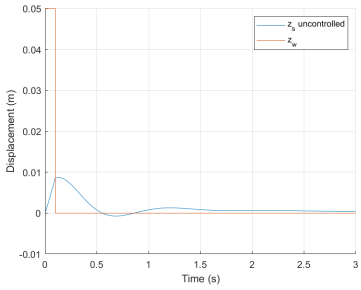

(b) Response to an impulse

3.2 Skyhook

In this part, a active control will be used to improve the efficiency of the system. The sprung damper will now be an active fore F. The system is represented figure **??**.

Figure 17: Controlled two degree of freedom system

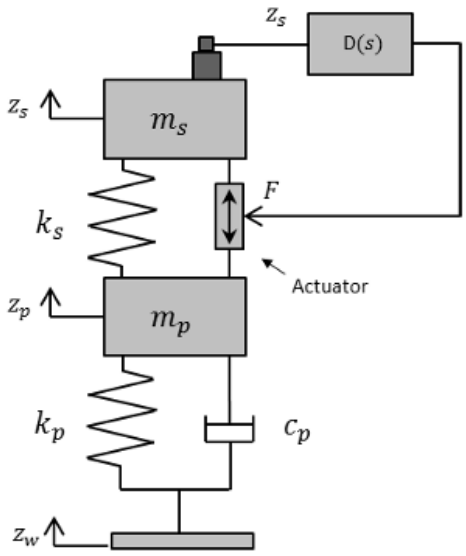

The controller is chosen to be in the form of a skyhook controller, $D(s) = -Ts$.

To simulate this system in simulink, we can represent this system in the state space. We have :

$$X = \begin{bmatrix} z_s \\ \dot{z}_s \\ z_p \\ \dot{z}_p \end{bmatrix} \tag{13}$$

Therefore the dynamic of the controlled system can be written :

$$\dot{X} = \begin{bmatrix} 0 & 1 & 0 & 0 \\ -\frac{k_s}{m} & 0 & \frac{k_s}{m_s} & 0 \\ 0 & 0 & 0 & 1 \\ \frac{k_s}{m_p} & 0 & -\frac{k_s+k_p}{m_p} & \frac{-c_p}{m_p} \end{bmatrix} \cdot X + \begin{bmatrix} 0 & 0 & 0 \\ 0 & 0 & \frac{1}{m_s} \\ 0 & 0 & 0 \\ \frac{k_p}{m_p} & \frac{c_p}{m_p} & -\frac{1}{m_p} \end{bmatrix} \cdot \begin{bmatrix} z_w \\ \dot{z_w} \\ F \end{bmatrix} \tag{14}$$

This state space problem was implemented in simulink for a skyhook controller. The simulink architecture is represented figure **??**.

Figure 18: Simulink model of the controlled two degree of freedom system

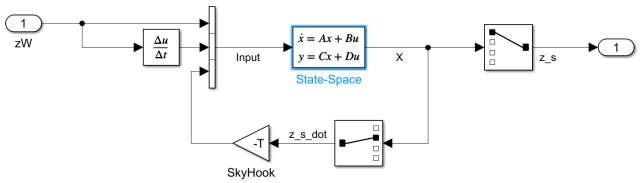

The parameter T requires some tuning. After several attempts, the parameter value $T = 0.1$ is optimal for scenarios 1 and 2. The response to these scenarios are

reprensented figure 19.

Figure 19: Response to different inputs signals for the skyhook controlled 2DOF system

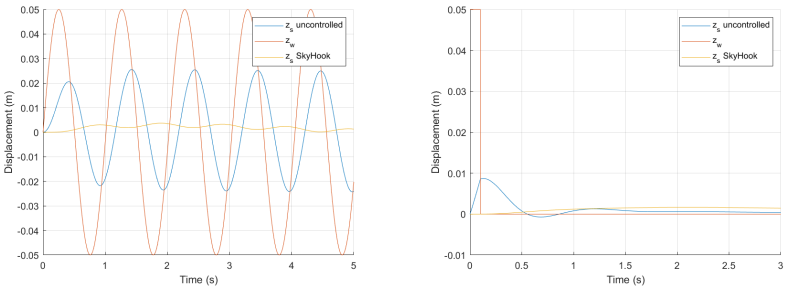

(a) Response to a sinusoidal signal

(b) Response to an impulse

This controller is very efficient to reduce the amplitude of the sinusoidal signal, and reduces significantly the overshoot with the impulse. The system is still underdamped and the natural frequency is the same. However, no values of T were found that meets also the requirement to damp out faster than the damped passive system.

4 Control of bounce and pitch for a simple vehicle model using Skyhook and H_∞

When designing the comfort feature of a vehicle, the two most relevant DOFs (degrees of freedom) are the bounce (z) and the pitch (θ). Thus, a vehicle model including these two DOFs is introduced in this Section, and different control strategies are investigated:

- Passive suspension system;
- Active suspension system with a Skyhook strategy;
- Active suspension system with a H_∞ controller.

The vehicle model with passive suspension is shown in the image below, where also the displacements due to the road irregularity (z_{w1} and z_{w2}) are represented, for the sake of completeness:

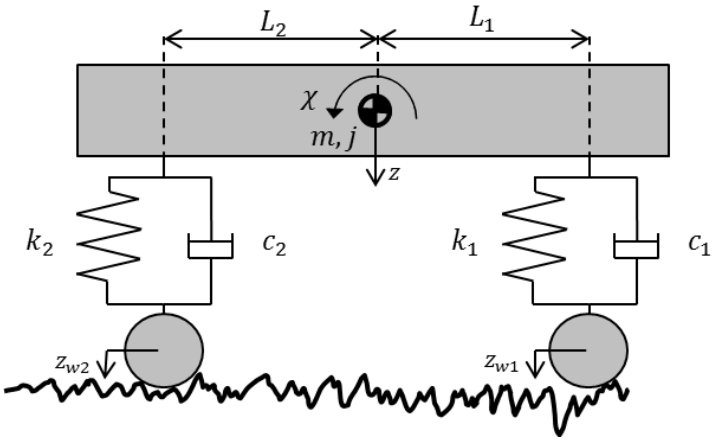

Figure 20: Two degrees of freedom vehicle (bounce and pitch) – passive suspension

Also the vehicle model controlled by means of active suspension is shown in the image below:

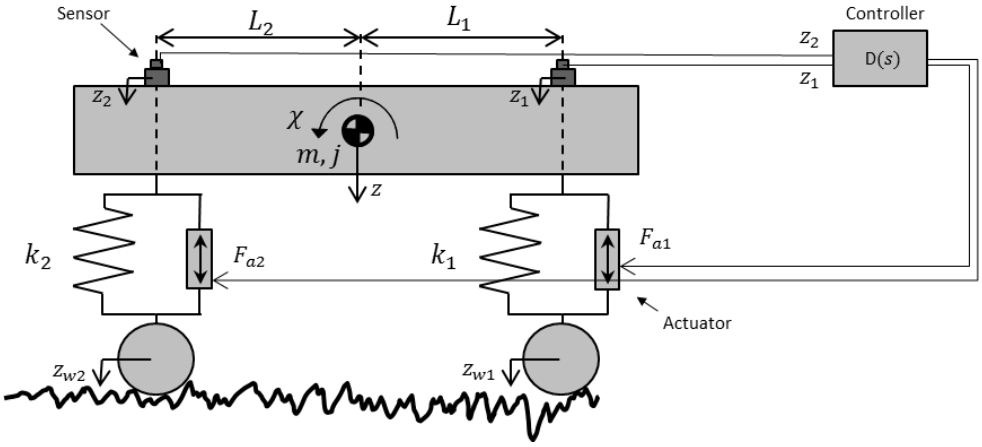

Figure 21: Two degrees of freedom vehicle (bounce and pitch) – active suspension

The characteristic parameters of this model are listed in the following table:

Table 1: Vehicle parameters

Parameter	Value	Unit measure
Mass (m)	$22 \cdot 10^3$	kg
Pitch inertia (J_y)	$700 \cdot 10^3$	$kg \cdot m^2$
Damping factor (c)	$40 \cdot 10^3$	$N \cdot s/m$
Spring stiffness (K)	$600 \cdot 10^3$	N/m
Front axle to COG distance (L_1)	6	m
Rear axle to COG distance (L_2)	6	m

4.1 Damped passive system

The first step in the analysis of this system consists of retrieving the equations of motion relative to the two main DOFs z and θ. The Lagrangian approach is adopted in this case, characterized by the following equation:

$$\frac{d}{dt}\left(\frac{\partial W}{\partial \dot{q}_i}\right) - \frac{\partial W}{\partial q_i} + \frac{\partial F}{\partial \dot{q}_i} = F_e \tag{15}$$

where:

- $W = E_k - E_u$ is the work, E_k is the kinetic energy and E_u is the potential energy;
- q_i is the degree of freedom in account;
- F is the dissipative energy, for instance the energy stored in the dampers;
- F_e are the external forces.

On the left-hand side of the equation, the energetic terms are considered in absolute value, but the displacement of the elements must be computed taking into account the positive definition of the DOFs. Instead, on the right-hand side, the external force contributions are considered positive when directed against the directions of the positively defined DOFs orientations. The same principle holds for the forces generating torques.
Thus, developing the Lagrangian Equation 15:

$$E_k = \frac{1}{2} \cdot m \cdot \dot{z}^2 + \frac{1}{2} \cdot J_y \cdot \dot{\theta}^2 \tag{16}$$

$$E_u = \frac{1}{2} \cdot K_1 \cdot (L_1 \cdot \theta - z)^2 + \frac{1}{2} \cdot K_2 \cdot (L_2 \cdot \theta + z)^2 \tag{17}$$

$$F = \frac{1}{2} \cdot c_1 \cdot (L_1 \cdot \dot{\theta} - \dot{z})^2 + \frac{1}{2} \cdot c_2 \cdot (L_2 \cdot \dot{\theta} + \dot{z})^2 \tag{18}$$

$$\begin{cases} q_i = z: \ F_e = K_1 \cdot z_{w1} + K_2 \cdot z_{w2} + c_1 \cdot \dot{z}_{w1} + c_2 \cdot \dot{z}_{w2} \\ q_i = \theta: \ F_e = -K_1 \cdot L_1 \cdot z_{w1} + K_2 \cdot L_2 \cdot z_{w2} - c_1 \cdot L_1 \cdot \dot{z}_{w1} + c_2 \cdot L_2 \cdot \dot{z}_{w2} \end{cases} \tag{19}$$

The Lagrangian equation is solved for both the q_i DOFs z and θ:

$$\begin{aligned} \ddot{z} = & -\frac{K_1 + K_2}{m} \cdot z - \frac{c_1 + c_2}{m} \cdot \dot{z} + \frac{K_1 \cdot L_1 - K_2 \cdot L_2}{m} \cdot \theta + \frac{c_1 \cdot L_1 - c_2 \cdot L_2}{m} \cdot \dot{\theta} + \\ & + \frac{K_1}{m} \cdot z_{w1} + \frac{K_2}{m} \cdot z_{w2} + \frac{c_1}{m} \cdot \dot{z}_{w1} + \frac{c_2}{m} \cdot \dot{z}_{w2} \end{aligned} \tag{20}$$

$$\begin{aligned} \ddot{\theta} = & \frac{K_1 \cdot L_1 - K_2 \cdot L_2}{J_y} \cdot z + \frac{c_1 \cdot L_1 - c_2 \cdot L_2}{J_y} \cdot \dot{z} - \frac{K_1 \cdot L_1^2 + K_2 \cdot L_2^2}{J_y} \cdot \theta - \frac{c_1 \cdot L_1^2 + c_2 \cdot L_2^2}{J_y} \cdot \dot{\theta} + \\ & - \frac{K_1 \cdot L_1}{J_y} \cdot z_{w1} + \frac{K_2 \cdot L_2}{J_y} \cdot z_{w2} - \frac{c_1 \cdot L_1}{J_y} \cdot \dot{z}_{w1} + \frac{c_2 \cdot L_2}{J_y} \cdot \dot{z}_{w_2} \end{aligned} \tag{21}$$

Starting from these two sets of equations, it's possible to retrieve the state-space system characterizing the entire vehicle model.
The states of this system are:

$$\begin{Bmatrix} z \\ \dot{z} \\ \theta \\ \dot{\theta} \end{Bmatrix} \tag{22}$$

while its inputs are:

$$\begin{Bmatrix} z_{w1} \\ \dot{z_{w1}} \\ z_{w2} \\ \dot{z_{w2}} \end{Bmatrix} \tag{23}$$

and the desired outputs are:

$$\begin{Bmatrix} z \\ \theta \end{Bmatrix} \tag{24}$$

Starting from Equations 20 and 21, the Matrices A, B, C and D are retrieved:

$$A = \begin{bmatrix} 0 & 1 & 0 & 0 \\ -\frac{K_1+K_2}{m} & -\frac{c_1+c_2}{m} & \frac{K_1 \cdot L_1 - K_2 \cdot L_2}{m} & \frac{c_1 \cdot L_1 - c_2 \cdot L_2}{m} \\ 0 & 0 & 0 & 1 \\ \frac{K_1 \cdot L_1 - K_2 \cdot L_2}{J_y} & \frac{c_1 \cdot L_1 - c_2 \cdot L_2}{J_y} & -\frac{K_1 \cdot L_1^2 + K_2 \cdot L_2^2}{J_y} & -\frac{c_1 \cdot L_1^2 + c_2 \cdot L_2^2}{J_y} \end{bmatrix} \tag{25}$$

$$B = \begin{bmatrix} 0 & 0 & 0 & 0 \\ \frac{K_1}{m} & \frac{c_1}{m} & \frac{K_2}{m} & \frac{c_2}{m} \\ 0 & 0 & 0 & 0 \\ -\frac{K_1 \cdot L_1}{J_y} & -\frac{c_1 \cdot L_1}{J_y} & \frac{K_2 \cdot L_2}{J_y} & \frac{c_2 \cdot L_2}{J_y} \end{bmatrix} \tag{26}$$

$$C = \begin{bmatrix} 1 & 0 & 0 & 0 \\ 0 & 0 & 1 & 0 \end{bmatrix} \tag{27}$$

$$D = \begin{bmatrix} 0 & 0 & 0 & 0 \\ 0 & 0 & 0 & 0 \end{bmatrix} \tag{28}$$

4.2 Skyhook

As done for the passive system, also for the active suspension system with Skyhook control strategy, the equations of motion are retrieved by means of the Lagrangian approach. The difference is that, at this time, the dissipative force term is not present anymore, but is substituted by the external force produced by the active suspension:

$$\begin{cases} q_i = z: \ F_e = K_1 \cdot z_{w1} + K_2 \cdot z_{w2} + F_{a1} + F_{a2} \\ q_i = \theta: \ F_e = -K_1 \cdot L_1 \cdot z_{w1} + K_2 \cdot L_2 \cdot z_{w2} - F_{a1} \cdot L_1 + F_{a2} \cdot L_2 \end{cases} \tag{29}$$

$$\ddot{z} = -\frac{K_1 + K_2}{m} \cdot z + \frac{K_1 \cdot L_1 - K_2 \cdot L_2}{m} \cdot \theta + \frac{K_1}{m} \cdot z_{w1} + \frac{K_2}{m} \cdot z_{w2} + \frac{F_{a1}}{m} + \frac{F_{a2}}{m} \tag{30}$$

$$\begin{aligned} \ddot{\theta} = & \frac{K_1 \cdot L_1 - K_2 \cdot L_2}{J_y} \cdot z - \frac{K_1 \cdot L_1^2 + K_2 \cdot L_2^2}{J_y} \cdot \theta - \frac{K_1 \cdot L_1}{J_y} \cdot z_{w1} + \frac{K_2 \cdot L_2}{J_y} \cdot z_{w2} + \\ & - \frac{F_{a1} \cdot L_1}{J_y} + \frac{F_{a2} \cdot L_2}{J_y} \end{aligned} \tag{31}$$

As done in the previous Section, also here the state-space system is retrieved, considering the same states, but with input:

$$\begin{Bmatrix} z_{w1} \\ z_{w2} \\ F_{a1} \\ F_{a2} \end{Bmatrix} \tag{32}$$

and with output:

$$\begin{Bmatrix} \dot{z} \\ \dot{\theta} \end{Bmatrix} \tag{33}$$

Eventually the matrices A, B, C and D are retrieved:

$$A_s = \begin{bmatrix} 0 & 1 & 0 & 0 \\ -\frac{K_1+K_2}{m} & 0 & \frac{K_1 \cdot L_1 - K_2 \cdot L_2}{m} & 0 \\ 0 & 0 & 0 & 1 \\ \frac{K_1 \cdot L_1 - K_2 \cdot L_2}{J_y} & 0 & -\frac{K_1 \cdot L_1^2 + K_2 \cdot L_2^2}{J_y} & 0 \end{bmatrix} \tag{34}$$

$$B_s = \begin{bmatrix} 0 & 0 & 0 & 0 \\ \frac{K_1}{m} & \frac{K_2}{m} & \frac{1}{m} & \frac{1}{m} \\ 0 & 0 & 0 & 0 \\ -\frac{K_1 \cdot L_1}{J_y} & \frac{K_2 \cdot L_2}{J_y} & -\frac{L_1}{J_y} & \frac{L_2}{J_y} \end{bmatrix} \tag{35}$$

$$C_s = \begin{bmatrix} 0 & 1 & 0 & 0 \\ 0 & 0 & 0 & 1 \end{bmatrix} \tag{36}$$

$$D_s = \begin{bmatrix} 0 & 0 & 0 & 0 \\ 0 & 0 & 0 & 0 \end{bmatrix} \tag{37}$$

According to the Skyhook principle, the bounce and pitch motions of the vehicle body are always damped by means of the active suspension system, but are not influenced by the road irregularities, as in the case of the passive suspension. Thus, it's possible to express an equivalent force and torque related to the bounce and to the pitch rates relatively:

$$\begin{cases} F_z = -c_z \cdot \dot{z} \\ T_\theta = -c_\theta \cdot \dot{\theta} \end{cases} \tag{38}$$

with tuned equivalent damping values: $c_z = 18 \cdot 10^4$, $c_\theta = 7 \cdot 10^6$, as a function of the two forces delivered by the active suspension systems:

$$\begin{cases} F_z = F_{a1} + F_{a2} \\ T_\theta = -F_{a1} \cdot L_1 + F_{a2} \cdot L_2 \end{cases} \tag{39}$$

Rearranging this system of equations, it is possible to come up with the expression of the two active suspension forces as a function of the Skyhook force and torque:

$$\begin{cases} F_{a1} = \frac{F_z \cdot L_2 - T_\theta}{L_1 + L_2} \\ F_{a2} = \frac{F_z \cdot L_1 + T_\theta}{L_1 + L_2} \end{cases} \tag{40}$$

It is interesting to notice how the Skyhook equivalent force and torque simultaneously affect the force response on each active suspension system.

The architecture of how this controller has been implemented in Simulink is shown below:

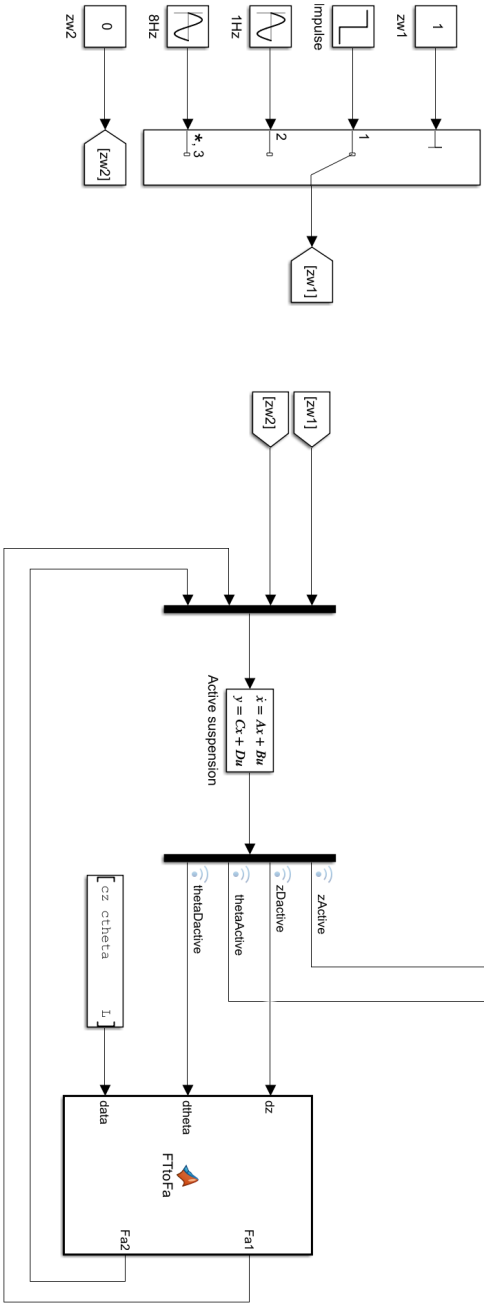

Figure 22: Skyhook Simulink architecture

4.3 H_∞ controller

A key feature of the H_∞ controller is the possibility to attenuate the system frequency response at its natural frequencies. Thus, it is crucial to understand what the natural frequencies associated with the bounce and with the pitch motions are. To do so, starting from the Skyhook state-space, the two relative transfer functions

are extracted by means of Matlab, and their magnitude response as a function of the frequency is reported below:

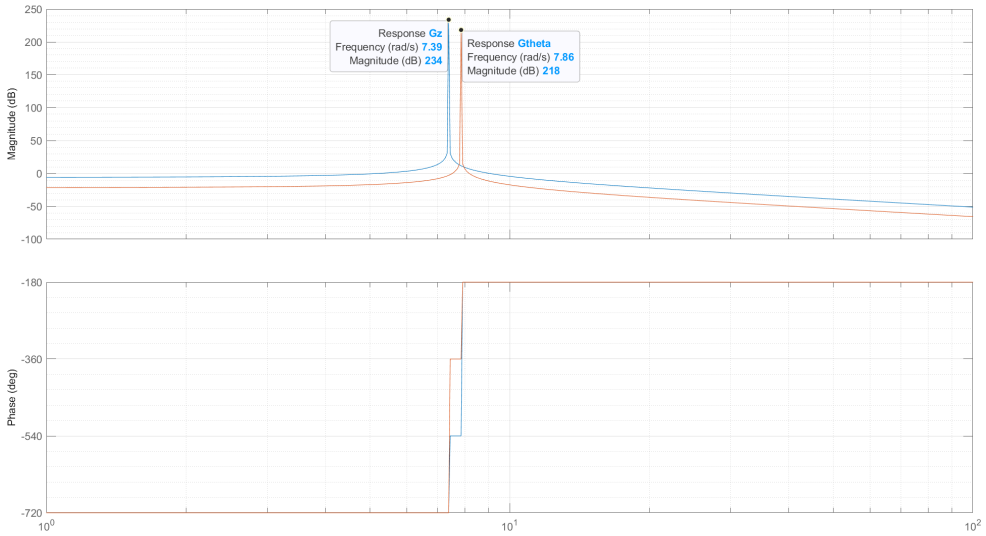

Figure 23: Frequency response

From this graph, the two natural frequencies are extracted in correspondence with the magnitude peaks:

$$\omega_{n,\,z} = 7.39 rad/s, \quad \omega_{n,\,\theta} = 7.86 rad/s$$

Then, these two values are used to calculate the poles characterizing the weighting function for the bounce and for the pitch:

$$W_i(s) = \frac{k_i \cdot s_1 \cdot s_2}{(s - s_1) \cdot (s - s_2)} \tag{41}$$

where:

- i stands for the considered DOF (z or θ);
- k_i are the gains influencing the command input activity (tuned values: $k_z = 1 \cdot 10^{-1}$, $k_\theta = 3.75 \cdot 10^2$);
- $s_{1,\,2} = -\varepsilon \pm i\sqrt{\omega_{n,\,i}^2 - \varepsilon^2}$ are the two poles of the weighting function;
- ε is an arbitrary small value selected to be 1.

Later on, these two weighting functions are coupled with the other two relative to the actuators force:

$$W_{a1} = W_{a2} = \frac{0.00175 \cdot s + 1}{0.00025 \cdot s + 1} \tag{42}$$

to extend the open loop system, controlled by means of the H_∞ controller K, as depicted in the following image:

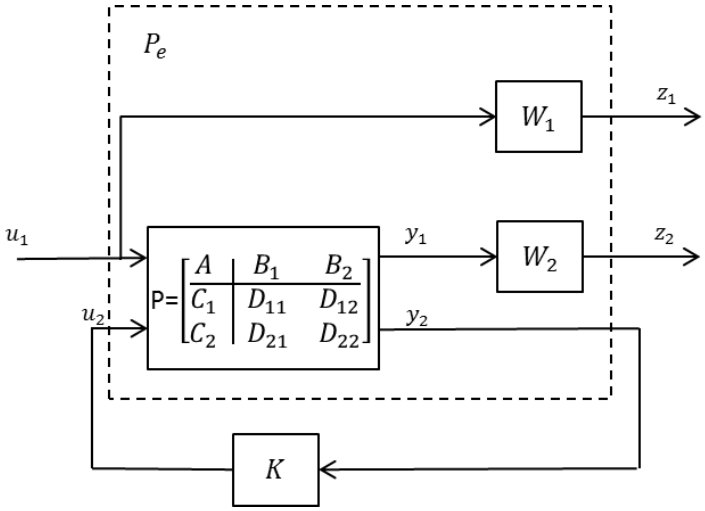

Figure 24: Extended open loop system under control of K

Starting from this control system, in the final Simulink architecture, the equivalent closed loop system is implemented:

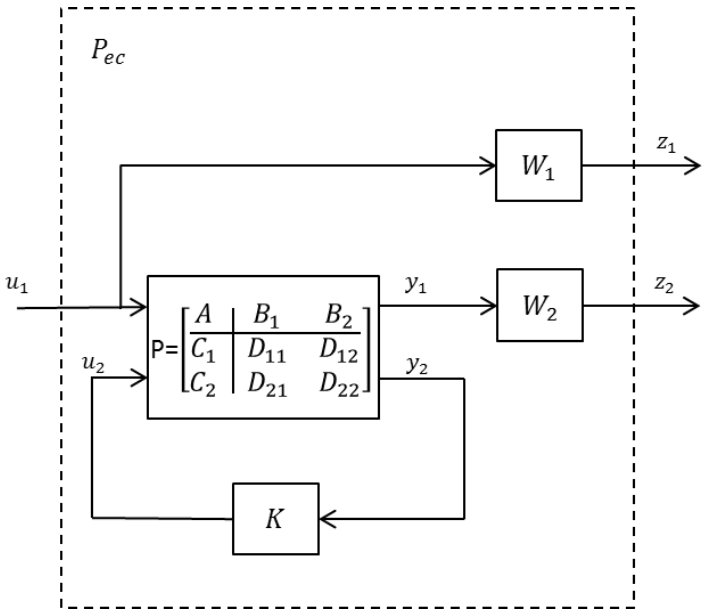

Figure 25: Extended closed loop system

where the two outputs are the ones pointed by the C_s matrix, indicated in Equation 33.

4.4 Chapter summary

Now that all the different control systems, both passive and active, for the 2 DOFs (bounce and pitch) vehicle model have been defined, it is possible to undertake a comparison of their performance and a sensitivity analysis for the different vehicle parameters.

Starting with the performance analysis, 3 different scenarios are simulated:

- Impulse input signal with an amplitude of $z_{w1} = 0.03m$;
- Sinusoidal input signal with amplitude of $z_{w1} = 0.01m$ and frequency of $f = 1Hz$;
- Sinusoidal input signal with amplitude of $z_{w1} = 0.01m$ and frequency of $f = 8Hz$.

Considering the road irregularity at the rear axle always constant: $z_{w2} = 0m$.
In the following images, the bounce and pitch trends for the three different control strategies are represented, and also the force delivered by the actuators with the Skyhook strategy:

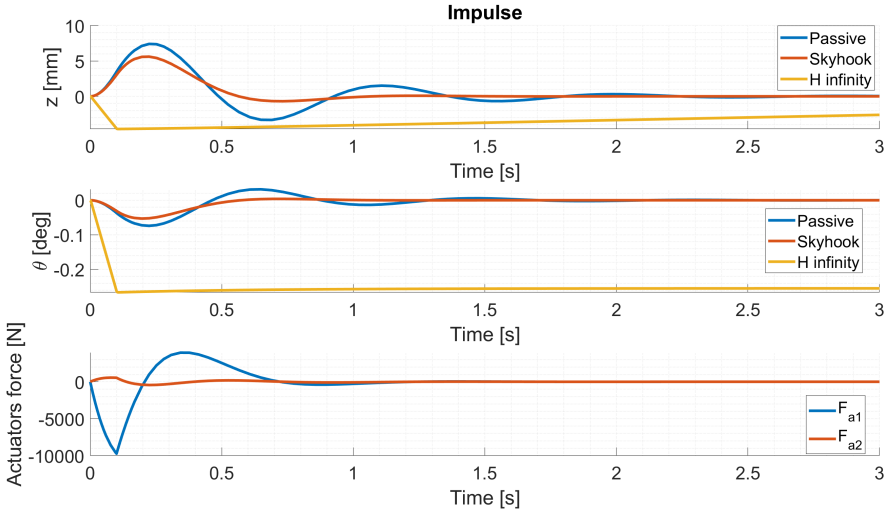

Figure 26: Comparison of the systems for an impulse input

In this scenario, as in all the next ones, the Skyhook performs much better than the passive system and of the H_∞ controller, significantly improving the comfort performance. Moreover, the actuator forces correctly respect the target limit of $10kN$, as in all the next cases.
The criticality of the H_∞ controller is that it keeps a pretty high steady-state error.

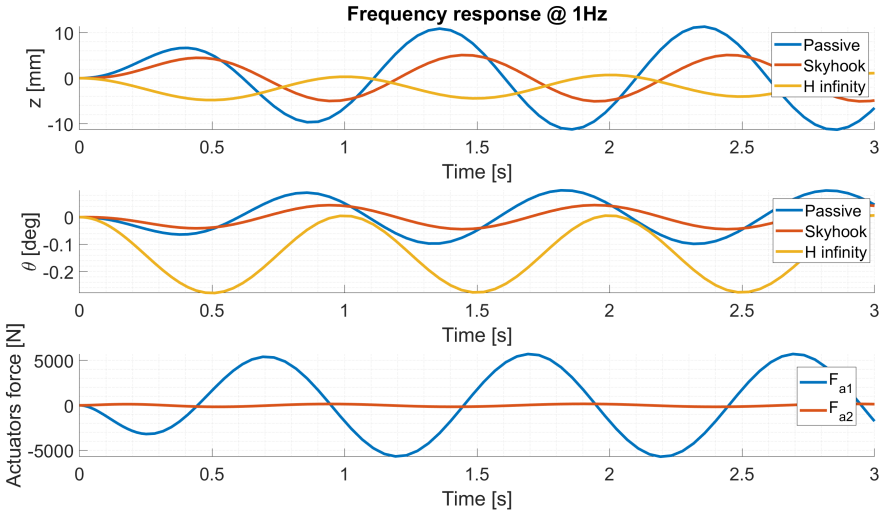

Figure 27: Comparison of the systems for a 1Hz sinusoidal input

The $1Hz$ frequency is the most close one to both the natural frequencies of the bounce and of the pitch. As expected by the H_∞ controller working principle, this strategy performs pretty well in this scenario, thanks to how the weighting functions have been designed around this frequency value.

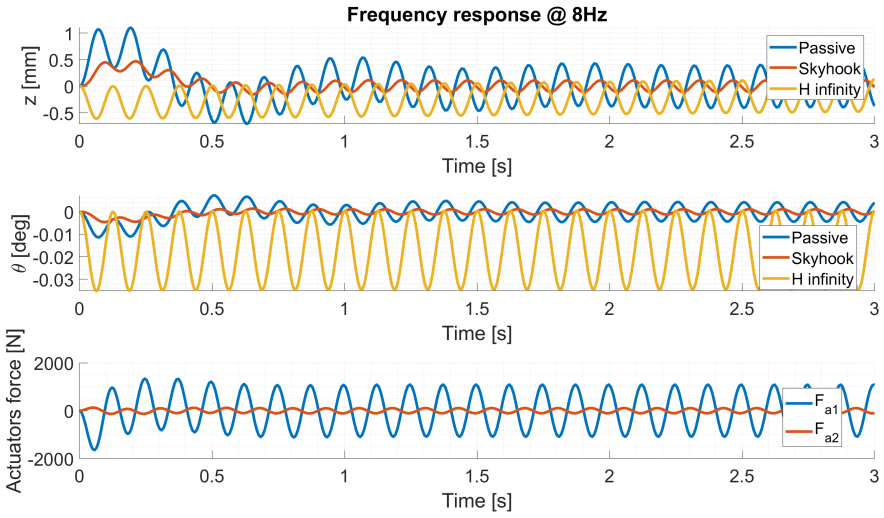

Figure 28: Comparison of the systems for an 8Hz sinusoidal input

Instead, in this higher frequency scenario, the performance of the H_∞ controller is more poor, but still better than the passive system.

Another interesting analysis is the sensitivity of the control strategies to the variation of vehicle parameters. In the first moment, only the vehicle mass influence is studied: bringing it from the standard value ($m = 22000kg$) to a value increased by the 15% ($m = 25300kg$):

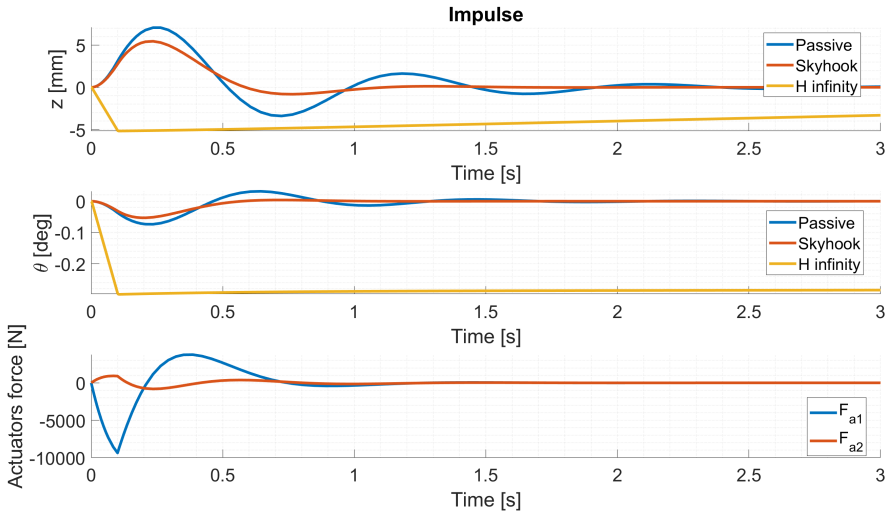

Figure 29: Impulse response with increased vehicle mass

The trends are pretty much the same as the ones shown in Figure 26, standing for a good stability, but the values with Skyhook of the maximum bounce and of the maximum front actuator force (in absolute value) are decreased respectively from $z = 5.6mm$ to $z = 5.4mm$, and from $F_{a1} = 9723N$ to $F_{a1} = 9365N$. In this case, the actuator force, being even decreased, is always within the target range.
This outcome is in accordance with the expectations: looking at the Equation 30, the mass term is always in the denominator, and increasing it a slower dynamic of the system is expected.

The last undertaken sensitivity analysis, instead, involves three different vehicle parameters simultaneously. Their combination is chosen in accordance with what could be the worst scenario for the control strategies stability:

- Vehicle inertia decreased by the 15%: from $J_y = 700 \cdot 10^3 kg \cdot m^2$ to $J_y = 595 \cdot 10^3 kg \cdot m^2$;
- Damping decreased by 15%: from $c = 40 \cdot 10^3 N \cdot s/m$ to $c = 34 \cdot 10^3 N \cdot s/m$;
- Stiffness increased by the 5%: from $K = 600 \cdot 10^3 N/m$ to $K = 630 \cdot 10^3 N/m$.

The resulting simulation with these parameters is shown here:

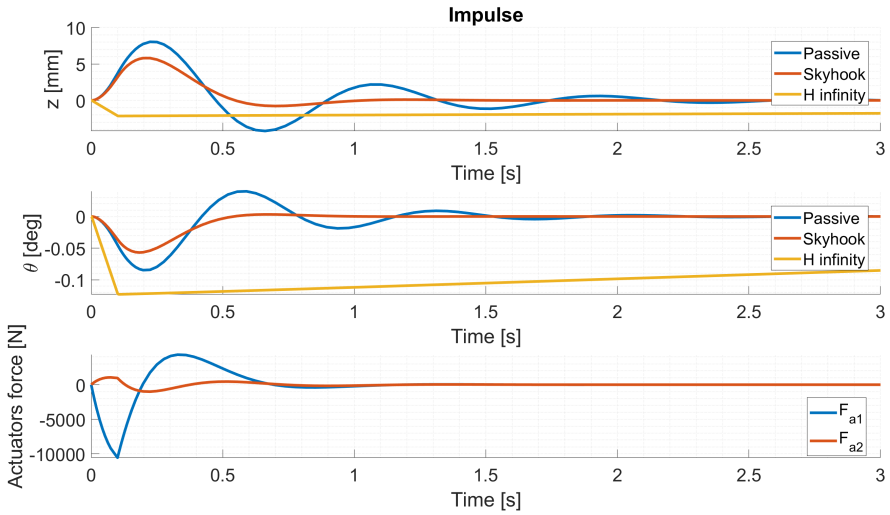

Figure 30: Impulse response with multiple vehicle parameters changes

The expectation is that a less dampened vehicle requires a higher force to dissipate the kinetic energy. Also the lower inertia should cause a faster dynamic, for the same principle explained previously, according to Equation 31.
According to these expectations, with respect to the standard values previously introduced ($\theta = 0.53°$ for the maximum pitch angle), the maximum pitch angle increases by the 8%, and the maximum front actuator force increases by the 9%.